

A Direct Torque-Controlled Interior Permanent-Magnet Synchronous Motor Drive Without a Speed Sensor

Muhammed Fazlur Rahman, *Senior Member, IEEE*, L. Zhong, Md. Enamul Haque, *Member, IEEE*, and M. A. Rahman, *Fellow, IEEE*

Abstract—This paper reports results of further investigation of the so-called direct torque control (DTC) technique to an interior permanent magnet (IPM) synchronous motor drive. This torque control technique for IPM motors requires no dq -axes current controllers and coordinate transformation networks. A completely sensorless IPM motor drive with DTC, which uses a new speed estimator from the stator flux linkage vector and the torque angle, is presented. It is shown that including the torque angle in the estimation process results in a far more accurate transient speed estimator than what is reported in the existing literature.

Index Terms—Coordinate transformation, current control, direct torque control, interior permanent magnet motor, mechanical shaft sensor, rotor flux linkage, rotor reference frame, speed estimator, stator flux linkage.

I. INTRODUCTION

THE PRINCIPLE of direct torque control (DTC), which was recently developed for induction motors, has now been implemented on an interior permanent magnet (IPM) motor [1], [2]. The DTC technique is different from traditional methods of controlling torque where current controllers in a suitable reference frame are used to control the motor torque and fluxes [3], [4]. The DTC technique, in doing the same tasks, does away with these current controllers or the indirect torque controllers, so to speak. The advantages of the DTC thus include the elimination of the dq -axes current controllers, associated coordinate transformation networks, and the rotor position sensor required for the coordinate transformation. With DTC for the IPM motor, control of torque is exercised through control of the amplitude and angular position of the stator flux vector relative to the rotor flux vector, the initial position of the latter being only required initially and quite approximately.

The relevant theory behind the development of the DTC for the interior magnet motor was elaborately described in [1]. In a subsequent paper [2], the controller was further improved to include the necessary trajectory controllers so that motor voltage and current limits could be employed and constant maximum torque and field weakening regimes were included. These implementations, however, included the shaft encoder for the speed control loop, although it was not used for the inner torque and flux loops. The encoder also supplied the initial rotor position, which is mandatory.

The presence of the shaft encoder for the above two purposes would tend to negate the main advantage of the DTC scheme, which is the elimination of the shaft position sensor. A true DTC scheme would not require any shaft sensor.

Techniques for determining the initial rotor position for an IPM motor without a mechanical sensor have been put forward recently [5], [6]. Since the DTC scheme proposed in references 1 and 2 require the initial position of the rotor to be known only approximately (i.e., with a resolution of 60 electrical degrees only), simple initial position detecting schemes can be easily included in the DTC scheme.

This paper reports results of further development of the DTC technique for IPM synchronous motors without requiring a mechanical speed sensor for the speed loop. Since the high-performance torque and flux control loops in the DTC scheme do not require rotor dq -current controllers and, hence, coordinate transformation networks, this development is, by definition, a sensorless technique.

In this paper, a technique of speed estimation from the stator flux vector φ_s and the torque angle δ , which are used for controlling the developed torque, in both steady-state and dynamic conditions of the drive, has been proposed and investigated. It is shown that if both of these two variables are used in the estimation, the rotor speed can be estimated with sufficient accuracy both for the steady-state and dynamic conditions of operation. A basis for a completely sensorless, fast dynamic response, IPM motor drive with DTC is thus presented.

II. REVIEW OF SENSORLESS POSITION AND SPEED ESTIMATION TECHNIQUES

Recent research on sensorless speed estimation techniques can be broadly classified into three categories, namely

- a) back-emf-based estimators;
- b) MRAS-based estimators;
- c) observer-based estimators.

The first category of algorithms is based on the estimation of stator flux linkage waveform, which is found from integrating the back emf [7]. These estimators work well at speeds above about 20% of the base speed. At low speed or at standstill, these estimators fail. Consequently, additional facilities are required to start the motor.

The second category is based on model reference adaptive (MRAS) techniques which uses a speed independent model (the reference model) and a speed-dependent model. The error from

Manuscript received September 17, 2001; revised August 29, 2002.

M. F. Rahman is with the School of Electrical Engineering and Telecommunication, The University of New South Wales, Sydney NSW 2052, Australia.

Digital Object Identifier 10.1109/TEC.2002.805200

the two is forced to zero by an adjusting mechanism, which gives the estimated speed [8].

The third category uses observer theory where an augmented linearised state-space model is used. States of the drive, including the rotor speed, are estimated by comparing variables in the model and from experimental data [9]. Extended Kalman filtering techniques are popular.

Techniques in the second and third categories are computationally intensive. In the DTC, which calls for fast sampling times of the order of a few tens of microseconds, the algorithms in category A are very attractive since complete information on stator flux linkage φ_s and load angle δ are continuously available at all times. Knowledge of δ is particularly useful, as it improves the accuracy of speed estimation of the IPM motor as is shown in latter sections.

III. LIMITATIONS OF STATOR FLUX LINKAGE-BASED SPEED ESTIMATORS

The traditional methods for speed estimation based on the stator flux linkage have the problems that a) they are only valid for the steady state, b) the stator flux linkage is estimated from the integration of the stator voltage which suffer from the dc offset and drift of the feedback signals, and c) that the stator flux linkage is a sinusoidal function of time. These also assume, as in [7], that the stator flux linkage remains constant regardless of the change in torque. This is very restrictive for the IPM motor. The angular displacement between the stator and rotor flux linkage vectors δ changes as the stator and rotor flux vectors rotate, when the torque changes transient state. Consequently, the rotor flux linkage vector rather than the stator flux linkage vector should be used for estimating the rotor speed. In the absence of any mechanical sensor, the rotor flux linkage vector must be determined from the estimated stator flux linkage vector φ_s and the load angle δ .

IV. PROPOSED SCHEME BASED ON ROTOR FLUX VECTOR

This paper proposes a scheme in which the torque angle δ is subtracted from the angle of the stator flux linkage φ_s , in order to obtain the rotor flux position continuously. The DTC scheme for the IPM motor is naturally suited for this technique since the full information on δ is always available within the DTC controller. The theoretical basis of this proposed estimator is given below.

The DTC scheme switches six voltage vectors to the three-phase IPM motor as indicated in Fig. 1.

The stator flux linkage of any three-phase stator winding can be expressed in the stationary reference frame as

$$\varphi_s = \int (\mathbf{v}_s - R\mathbf{i}_s) dt. \quad (1)$$

During the switching interval, each voltage vector \mathbf{v}_s is constant and (1) is then rewritten as in (2).

$$\varphi_s = \mathbf{v}_s t - \int R\mathbf{i}_s dt + \varphi_s|_{t=0} \quad (2)$$

where $\varphi_s|_{t=0}$ is the initial stator flux vector at $t = 0$ and \mathbf{v}_s is the applied stator voltage vector. Components of the stator voltage vectors \mathbf{v}_s along the stator D - and Q -axes, v_D and v_Q ,

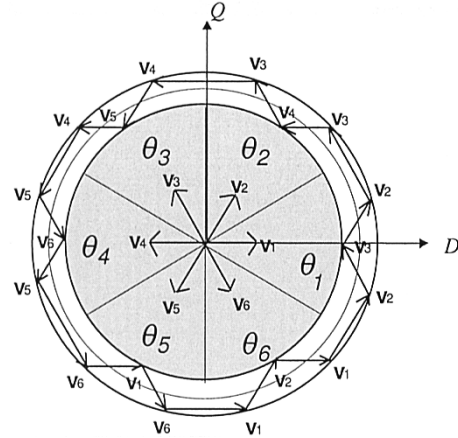


Fig. 1. Voltage vectors for DTC.

respectively, in terms of the dc link voltage of the inverter V_d are given in Table I. The D - and Q -axes stator flux linkages, φ_D and φ_Q , are then given by

$$\begin{aligned} \varphi_{D(k)} &= \varphi_{D(k-1)} + \{v_{D(k-1)} - R\bar{i}_{D(k)}\} T_s \\ \varphi_{Q(k)} &= \varphi_{Q(k-1)} + \{v_{Q(k-1)} - R\bar{i}_{Q(k)}\} T_s \end{aligned} \quad (3)$$

where

$$\bar{i}_{D(k)} = \frac{i_{D(k-1)} + i_{D(k)}}{2}, \quad \bar{i}_{Q(k)} = \frac{i_{Q(k-1)} + i_{Q(k)}}{2}$$

where T_s is the sampling interval, and

i_D, i_Q are the stator currents in the D and Q axes, and variables k and $k - 1$ in brackets refer to the k th and $k - 1$ th sampling instants, respectively.

The stator flux vector is then given by

$$\varphi_{s(k)} = \sqrt{\varphi_{D(k)}^2 + \varphi_{Q(k)}^2} \angle \tan^{-1} \left(\frac{\varphi_{Q(k)}}{\varphi_{D(k)}} \right) = \hat{\varphi}_{s(k)} \angle \varphi_{s(k)}. \quad (4)$$

The motor developed torque in terms of the stator fluxes is given by

$$T(k) = \frac{3}{2} P \{ \varphi_{D(k)} i_{Q(k)} - \varphi_{Q(k)} i_{D(k)} \} \quad (5)$$

where P is the number of pole pairs. The motor developed torque, in terms of the stator and rotor flux linkage amplitudes is also given as

$$T(k) = \frac{3p\hat{\varphi}_{s(k)}}{4L_d L_q} \cdot [2\varphi_f L_q \sin\{\delta(k)\} - \hat{\varphi}_{s(k)} (L_q - L_d) \sin 2\{\delta(k)\}] \quad (6)$$

where φ_f is the stator flux linkage due to the rotor permanent-magnet excitation only.

Knowing the torque $T(k)$ from (5), the torque angle $\delta(k)$ can be found from (6). The rotor position is then given by $\angle \varphi_{s(k)} - \delta(k)$, which, after differentiation and some filtering, gives the speed signal. The proposed speed estimator is thus based on the following steps and inputs:

- 1) the stator flux linkage φ_s : Since the stator flux linkage is controlled within the DTC, its position is known;

TABLE I
DQ-AXES VOLTAGES

	V_1	V_2	V_3	V_4	V_5	V_6
v_D	V_d	$0.5 V_d$	$-0.5 V_d$	$-V_d$	$-0.5 V_d$	$0.5 V_d$
v_Q	0	$0.866 V_d$	$0.866 V_d$	0	$-0.866 V_d$	$-0.866 V_d$

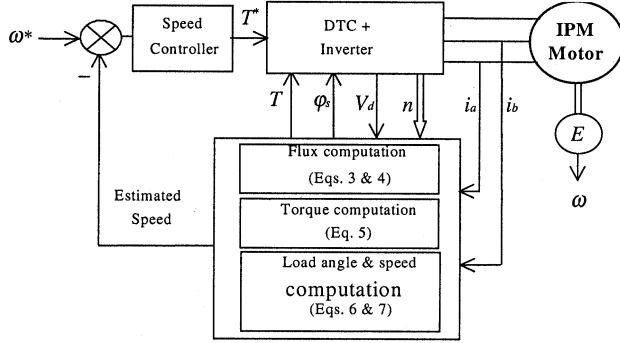


Fig. 2. Experimental DTC drive system.

- 2) the actual developed torque from (5): The torque angle δ can be calculated from the torque (6), [or it may be obtained from a lookup table representing (6)];
- 3) the rotor position: This is obtained from the stator flux position and the torque angle;
- 4) change of the rotor position in certain time interval gives the rotor speed: This must be filtered to obtain a smooth speed signal;
- 5) the initial starting position of the rotor. It is obtained from a simple test at start [5].

V. DRIVE SYSTEM DESCRIPTION

The drive system consists of a 415-V, three-phase, four-pole, 1-kW, IPM motor of Table II, driven from an IGBT inverter which is interfaced with a TMS320C31 digital signal processor (DSP) board as indicated in Fig. 2. The inverter dc-link voltage V_d , the applied voltage vector number n , and the two line currents i_a and i_b are also interfaced to the DSP board. The shaft encoder indicated is only for comparing the estimated speed with the actual measured speed. It is not used for torque control subsequently.

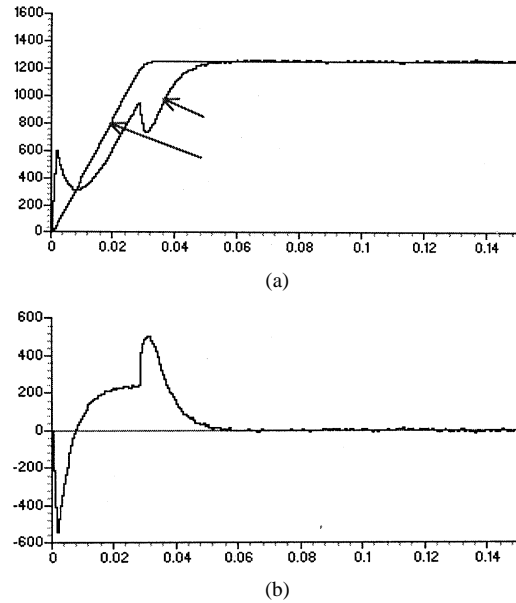
The DTC controller applies the voltage vectors V_n , ($n = 1-6$), as indicated in Fig. 1, according to the errors of the torque and flux controllers (hysteresis controllers). While the error of the speed controller readily defines the torque reference, the reference for the stator flux controller (within the DTC) is generated according to some desirable trajectory following properties for the motor of Table II.

VI. MODELING STUDIES

Three cases have been investigated through modeling, as given below. Constant maximum torque per ampere (MTPA) mode of operation has been selected in all three cases since this mode of operation is likely to be selected at low speeds where speed estimation is difficult. Furthermore, this mode of

TABLE II
PARAMETERS OF THE IPM MOTOR USED. (KOLLMORGEN MOTOR MODEL: B-402A)

Number of pole pairs	P	2
Stator resistance	R_s	5.8Ω
Magnet flux linkage	ϕ_f	0.377 Wb
d -axis inductance	L_d	0.0448 H
q -axis inductance	L_q	0.1024 H
Phase voltage	V	145 V
Phase current	I	3 A
Base speed	ω_b	1500 rpm
Rated torque	T_b	6.8 Nm

Fig. 3. (a) Estimated and actual speeds and (b) speed error in case A (estimation from ϕ_s alone). Modeling results.

operation subjects the motor to the highest dynamic response, so that the ability of the speed estimator to track the actual speed for this mode of operation is mainly of interest.

In order to evaluate the proposed speed estimator, modeling studies are undertaken for the following three cases.

A. Estimation of Rotor Speed From the Stator Flux Linkage ϕ_s

In this case, the rotor speed is estimated from ϕ_s alone and the speed feedback signal for speed control is obtained from a 5000-counts/rev encoder (which is also modeled). The actual and estimated speed and the torque responses of the drive during acceleration from standstill to 1250 r/min are indicated in Fig. 3(a) and (b), respectively. When the motor starts, the stator

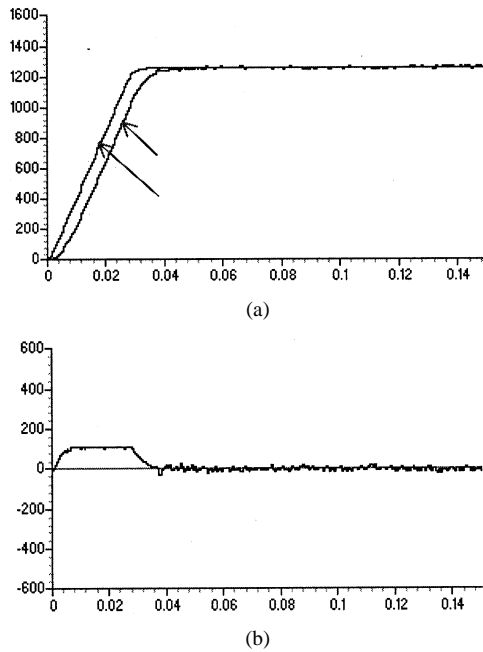


Fig. 4. (a) Estimated and actual speeds and (b) speed error in case B (estimation from $\angle\varphi_s - \delta$). Modeling results.

flux rotates very fast to produce a torque angle required for maximum torque. If we assume that the rotor speed is the same as the rotational speed of the stator flux, large errors occur at low speed, as shown in Fig. 3(a). When the rotor speed approaches its reference, the stator flux slows down or even rotates in the opposite direction (as required by the DTC) to reduce the torque. Large errors occur again since the rotor speed largely remains unchanged in the presence of large change in torque. These results confirm the limitations of the traditional stator flux-based speed estimators mentioned in Section III.

B. Estimation of Rotor Speed From Rotor Flux Position, $\angle\varphi_s - \delta$

In this case, the rotor speed is estimated from the rotor flux vector position $\angle\varphi_s - \delta$, which is obtained as described in Section IV. The actual speed signal is still obtained from the encoder (which is modeled), as in case A. The estimated and actual speeds for this case are indicated in Fig. 4.

In both cases A and B, the speed-controlled system does not use the speed signal from the estimator for closing the speed loop. The speed estimator operates offline (i.e., its output is not used in closing the speed loop).

C. Estimation of Rotor Speed From Rotor Flux Position, $\angle\varphi_s - \delta$; With Speed Feedback From the Estimator (Closed Loop)

The speed feedback signal in this case is obtained as in B; however, the speed estimator output (rather than the speed signal from the encoder) is now used in closing the speed loop. In other words, the encoder is now not required for the speed-controlled system. The following considerations, however, have been found to be very critical.

- 1) A filter must be used to obtain a smooth speed signal.

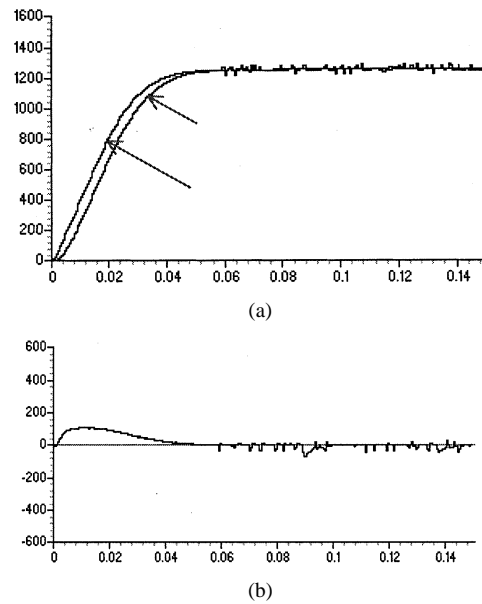


Fig. 5. (a) Estimated and actual speeds and (b) speed error in case C (speed loop closed with estimated speed). Modeling results.

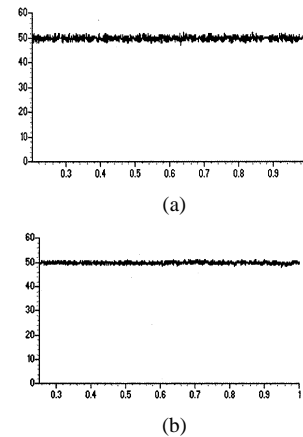


Fig. 6. Steady-state speed estimation at low speed, (a) with no load (b) with 50% rated load. Reference speed = 50 r/min.

- 2) The delay due to filtering is very critical, which may cause the system to become unstable.
- 3) Adequate limits to the error of the speed estimator in both transient and steady states must be in place.

Fig. 5 includes results of the estimated and actual speeds and flux and torque responses when the motor is accelerated from rest with the speed feedback signal derived from the estimator. From the results of Fig. 5, it is seen that the error in estimated speed both in the transient and steady-state is consistent with the results of Fig. 4.

With closed-loop speed control using the estimated speed for feedback, the steady-state speed tracks the speed reference very well, both when the drive is unloaded and 50% loaded. These are shown in Fig. 6. The reference speed for each case was 50 r/min (i.e., 3.3% of base speed). Fig. 7 indicates the effect of sudden application of 75% of rated load torque on the drive once it has settled to its final speeds of 1250 r/min (Fig. 7(a)) and 300 r/min (Fig. 7(b)). These results are indicative of the robustness of the speed estimator and of the drive system to an abrupt change in load torque.

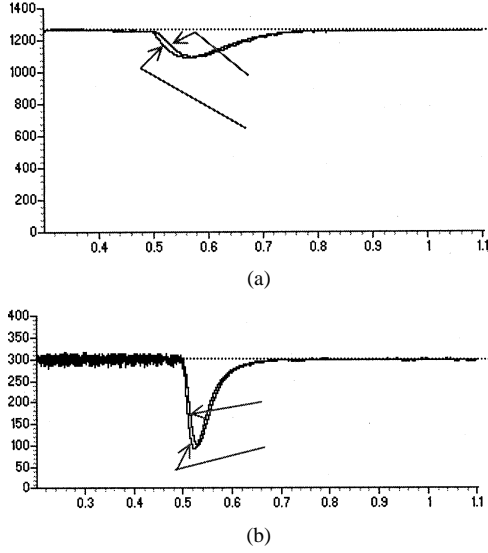


Fig. 7. Effect of load torque disturbance on estimated and actual speeds for the drive in case C. $\Delta T_L = 75\%$ of rated torque. Modeling results.

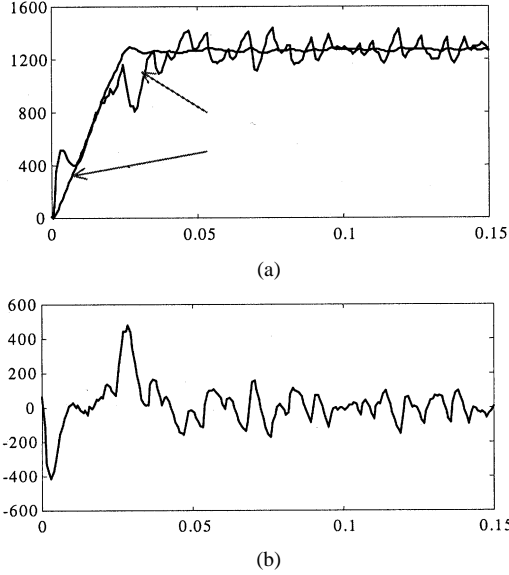


Fig. 8. (a) Estimated and actual speeds and (b) speed error in case A (estimation from φ_s alone).

VII. EXPERIMENTAL RESULTS

The DTC drive setup of Fig. 2, which is described in Section V, was used to implement and evaluate the mechanical sensorless speed observers presented in Section VI. In the results that follow, the terms *actual speed* now refer to the speed which is measured with the mechanical sensor (encoder). Fig. 8 shows estimated speed and the speed error against the actual speed when the drive is accelerated from zero speed to 1250 r/min along the MTPA trajectory. The speed estimator operates off-line. The magnitudes of the speed errors during the transient are seen to conform very closely to errors observed in modeling (Fig. 3). The oscillations in the estimated speed are due to the errors in the computations of φ_s , which use rather noisy signals.

The speed observer based on the rotor flux linkage vector [i.e., on $(\angle \varphi_s - \delta)$] gives much lower speed error, as shown by the experimental results of Fig. 9. The operating conditions of

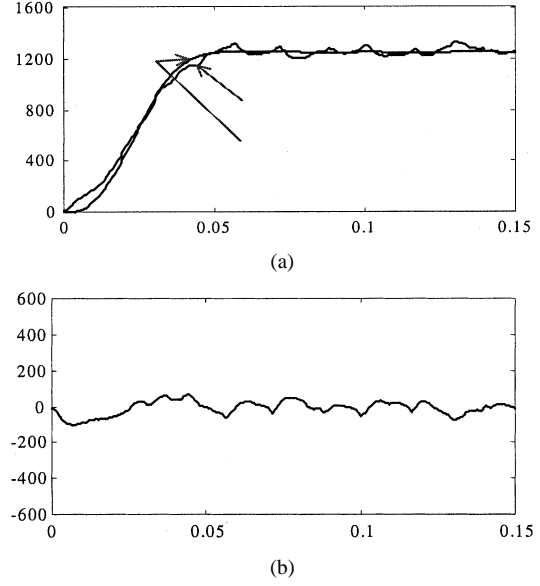


Fig. 9. (a) Estimated and actual speeds and (b) speed error in case B (estimation from $\angle \varphi_s - \delta$).

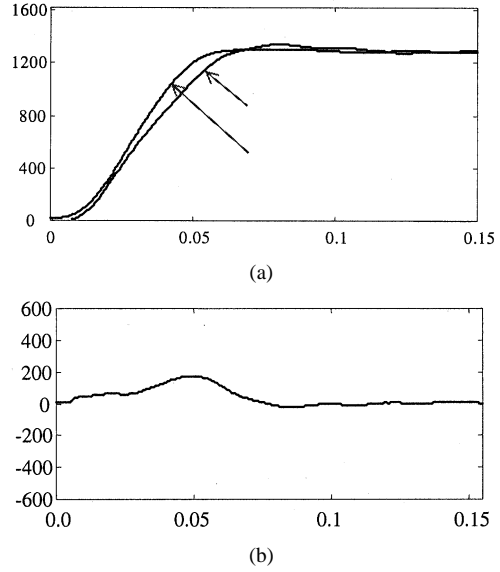


Fig. 10. (a) Estimated and actual speeds and (b) speed error in case C (speed loop closed with estimated speed).

the drive are similar to those of Fig. 8. Clearly, this observer is much more accurate than the one based on stator flux linkage.

When the speed loop is closed (Fig. 10) with the speed feedback derived from the modified observer of Fig. 9, the magnitudes of the speed error during the acceleration become larger but still much smaller than the error when only the stator flux linkage vector φ_s is used (refer to Fig. 8(b)).

The low-speed performance of the rotor flux-based speed observer was tested by setting the reference speed to 50 r/min (3.33% of base speed). The experimental results of Fig. 11 show the mean speed (50 r/min) with some speed ripples around this speed.

When the drive is subjected to some abrupt load, it slows down and recovers to the reference speed. The experimental results of Fig. 12 closely match the modeling results of Fig. 7 on the rejection of load disturbance.

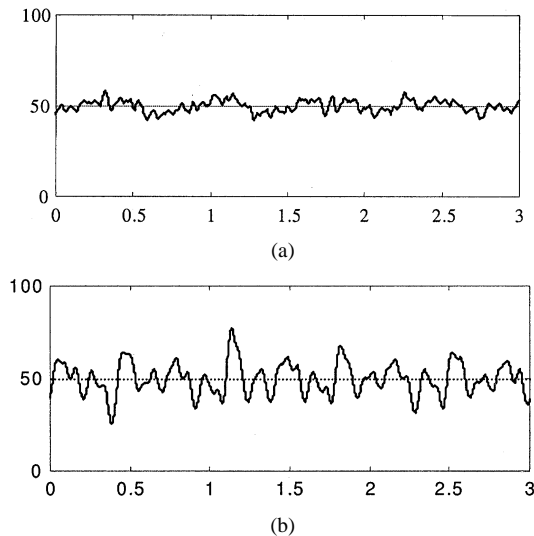


Fig. 11. Steady-state speed estimation at low speed, (a) with no load (b) with 30% rated load. Reference speed = 50 rev/min.

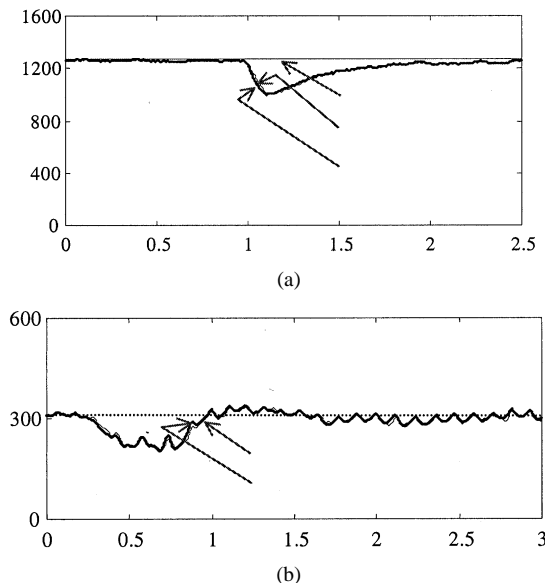


Fig. 12. Effect of load torque disturbance on estimated and actual speeds for the drive in case C. $\Delta T_L = 50\%$ of rated torque.

VIII. CONCLUSION

This paper has presented a speed control system for an IPM motor with an inner DTC which does not require a mechanical position sensor. The speed feedback is from a new estimator, which uses the rotor flux linkage vector rather than the stator flux linkage vector as hitherto used. A comparison of the two ways of estimating the rotor speed has also been presented. The enhanced accuracy of rotor flux-based speed estimator is clearly demonstrated. The suitability and robustness of the DTC scheme in obtaining a speed sensorless IPM motor drive is also demonstrated.

REFERENCES

- [1] L. Zhong, M. F. Rahman, and W. Y. Hu, "Analysis of direct torque control in permanent magnet synchronous motor drives," *IEEE Trans. Power Electron.*, vol. 12, pp. 528–536, May 1997.
- [2] M. F. Rahman, L. Zhong, and K. W. Lim, "A direct torque controlled interior magnet synchronous motor drive incorporating field weakening," in *Proc. 1997 IEEE Ind. Applicat. Soc. Annu. Meeting*, vol. 1, New Orleans, LA, Oct. 5–9, 1997, pp. 67–74.
- [3] T. M. Jahns, "Flux-weakening regime operation of an interior magnet synchronous motor drive," *IEEE Trans. Ind. Applicat.*, vol. 23, pp. 681–689, July/Aug. 1987.
- [4] B. K. Bose, "A high-performance inverter-fed drive system of an interior magnet synchronous machine," *IEEE Trans. Ind. Applicat.*, vol. 24, pp. 987–997, Sept./Oct. 1988.
- [5] M. E. Haque, L. Zhong, and M. F. Rahman, "A sensorless initial rotor position estimation scheme for a direct torque controlled interior permanent magnet synchronous motor drive," in *Proc. IEEE Appl. Power Electron. Conf. Expo.*, vol. 2, Anaheim, CA, Mar. 4–8, 2001, pp. 879–884.
- [6] P. B. Schmidt, M. L. Gasperi, G. Ray, and A. H. Wijanayake, "Initial rotor position detection of a non salient pole permanent magnet synchronous motor," in *Proc. 1997 IEEE Ind. Applicat. Soc. Annu. Meeting*, vol. 1, New Orleans, LA, Oct. 5–9, 1997, pp. 459–463.
- [7] R. Wu and G. R. Slemon, "A permanent magnet motor drive without a shaft sensor," *IEEE Trans. Ind. Applicat.*, vol. 27, no. 5, pp. 1005–1011, 1991.
- [8] M. N. Marwali and A. Keyhani, "A comparative study of rotor flux based MRAS and back EMF based MRAS speed estimators for speed sensorless vector control of induction machines," in *Proc. IEEE Ind. Applicat. Soc. Annu. Meeting*, vol. 1, 1997, pp. 160–166.
- [9] R. Dhaouadi, N. Mohan, and L. Norum, "Design and implementation of an extended Kalman filter for the state estimation of a permanent magnet synchronous motor," *IEEE Trans. Power Electron.*, vol. 6, pp. 491–497, July 1991.

Muhammed Fazlur Rahman (M'78–SM'94) received the B.S. degree in electrical engineering from the Bangladesh University of Engineering and Technology, Dhaka, in 1972 and the M.S. and Ph.D. degrees from the University of Manchester, Manchester, U.K., in 1995 and 1978, respectively.

He subsequently worked as a Systems Design Engineer at the General Electric Projects Company, Rugby, U.K., for two years before joining the National University of Singapore, in 1980. He joined the University of New South Wales, Australia, in 1988, as a Senior Lecturer. His research interests are in power electronics, motor control, and motion control systems.

Dr. Rahman is a member of the IEEE Power Electronics Society, Industry Applications Society, and Industrial Electronics Society.

L. Zhong received the B.E. degree in electronic engineering from Zhejiang University of Technology, Hangzhou, China, in 1985 and the M.E. and Ph.D. degree from the University of New South Wales, Australia, in 1994 and 1999, respectively.

His research interests are in power electronics and ac motor drives.

Md. Enamul Haque (M'97) was born in Bangladesh in 1970. He received the B.S. degree in electrical and electronic engineering from Bangladesh Institute of Technology, Rajshahi, in 1995, the M.Eng. degree in electrical engineering from the University of Technology Malaysia, in 1998, and is currently pursuing the Ph.D. degree at the University of New South Wales, Sydney, Australia.

His research interests are in analog and digital electronics, power electronics, and computer control of ac motor drives.

M. A. Rahman (SM'73–F'88) received the B.Sc.Eng. degree from the Bangladesh University of Engineering and Technology, Dhaka, in 1962, the M.Sc. degree from the University of Toronto, Toronto, ON, Canada, in 1965, and the Ph.D. degree from the University of Carleton, Ottawa, ON, in 1968.

Currently, he is a Research Professor at University of Newfoundland, Canada. His research interests are in power electronics, machines, power systems and digital protection.

Dr. Rahman received a number of awards from the IEEE, including the IAS Outstanding Achievement Award in 1992. He is a Fellow of the Institution of Electrical Engineers, U.K.